



# Transparent Large Strain Thermoplastic Polyurethane Magneto-active Nanocomposites

## Summary

Smart adaptive materials are an important class of materials which can be used in space deployable structures, morphing wings, and structural air vehicle components where remote actuation can improve fuel efficiency. Adaptive materials can undergo deformation when exposed to external stimuli such as electric fields, thermal gradients, radiation (IR, UV, etc.), chemical and electrochemical actuation, and magnetic field. Large strain, controlled and repetitive actuation are important characteristics of smart adaptive materials. Polymer nanocomposites can be tailored as shape memory polymers and actuators.

Magnetic actuation of polymer nanocomposites using a range of iron, iron cobalt, and iron manganese nanoparticles is presented. The iron-based nanoparticles were synthesized using the soft template (1) and Sun's (2) methods. The nanoparticles shape and size were examined using TEM. The crystalline structure and domain size were evaluated using WAXS. Surface modifications of the nanoparticles were performed to improve dispersion, and were characterized with IR and TGA. TPU nanocomposites exhibited actuation for ~2wt% nanoparticle loading in an applied magnetic field. Large deformation and fast recovery were observed. These nanocomposites represent a promising potential for new generation of smart materials.

# Transparent Large Strain Thermoplastic Polyurethane Magneto-active Nanocomposites

Mitra Yoonessi, Ileana Carpen, John Peck,  
Francisco Sola, Justin Bail, Bradley Lerch, Michael Meador

Ohio Aerospace Institute, Cleveland, OH  
University of Akron, Akron, OH  
Tennessee Tech University, TN  
NASA Glenn Research Center, Cleveland, OH



# Stimuli Responsive Materials- Polymer



## Smart Adaptive Materials Nanocomposites

Materials responding to external stimuli in controlled repetitive reproducible manner

### Magnetic actuation

Remote actuation by applying electromagnetic , or magnetostatic fields (wireless actuation)

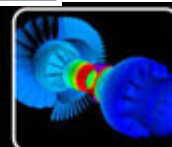
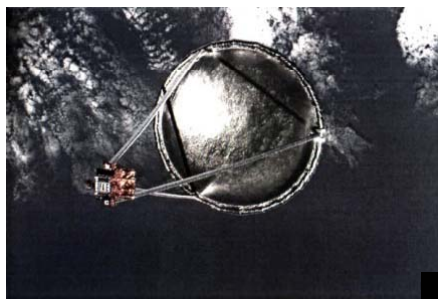
### Thermal actuation

shape memory – programmable materials to undergo deformation at specific temperature when thermal energy applied

### Electrical actuation

Actuators- hybrid materials that deform when electric voltage is applied

Improve efficiency  
Fan casing  
Space Flex. packaging  
Space Deployable structures



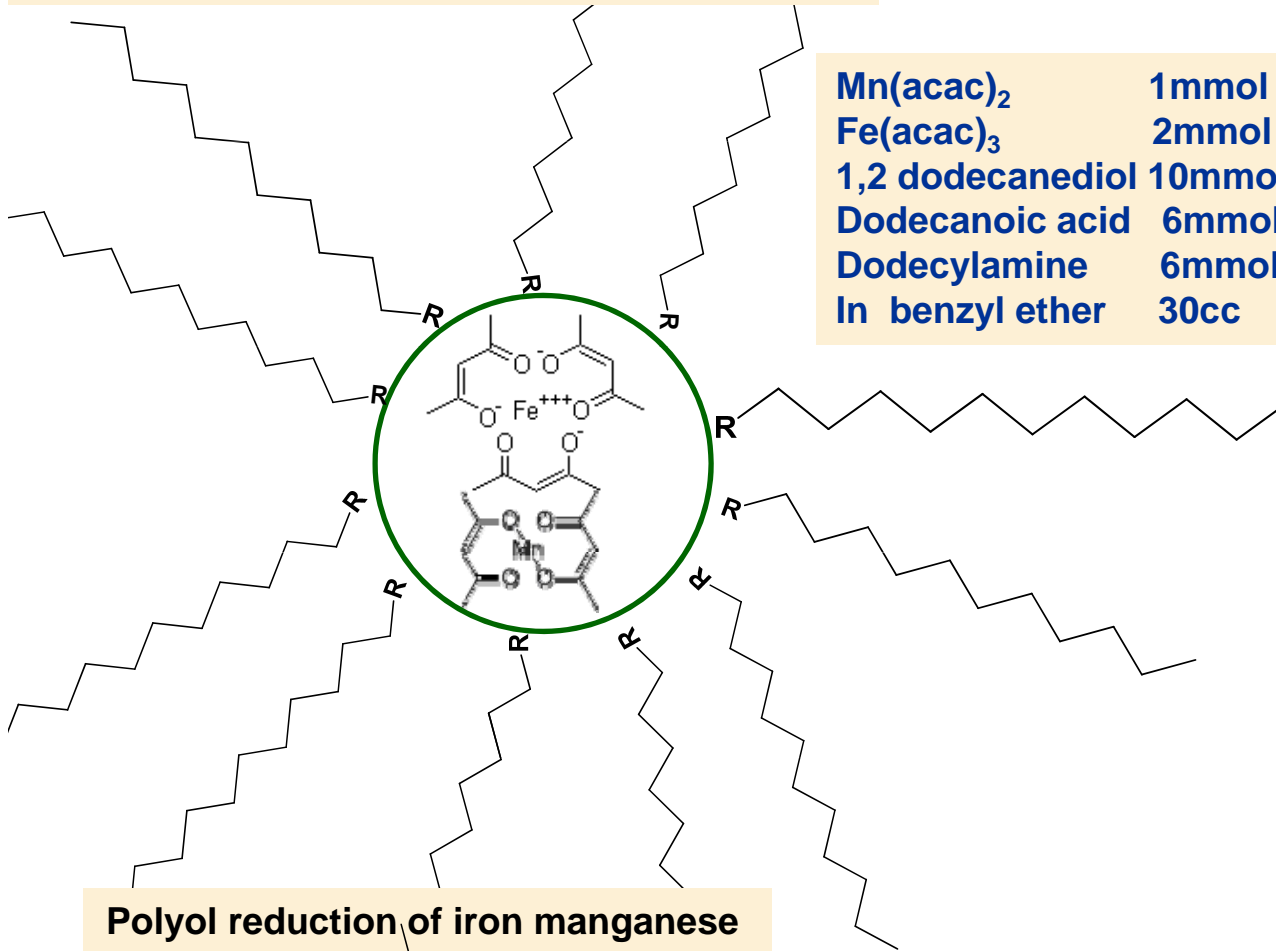
fundamental aeronautics

# Magnetic Nanoparticle Synthesis

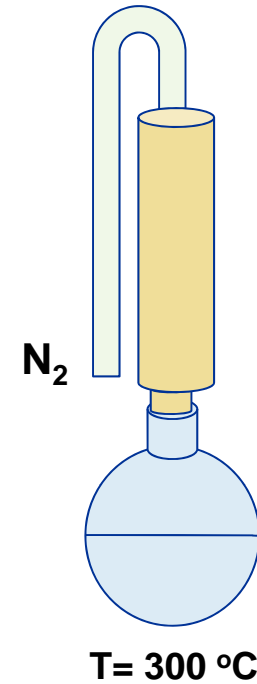


## Thermal decomposition method

Mn(acac) <sub>2</sub>	1mmol
Fe(acac) <sub>3</sub>	2mmol
1,2 dodecanediol	10mmol
Dodecanoic acid	6mmol
Dodecylamine	6mmol
In benzyl ether	30cc



Polyol reduction of iron manganese organic complex



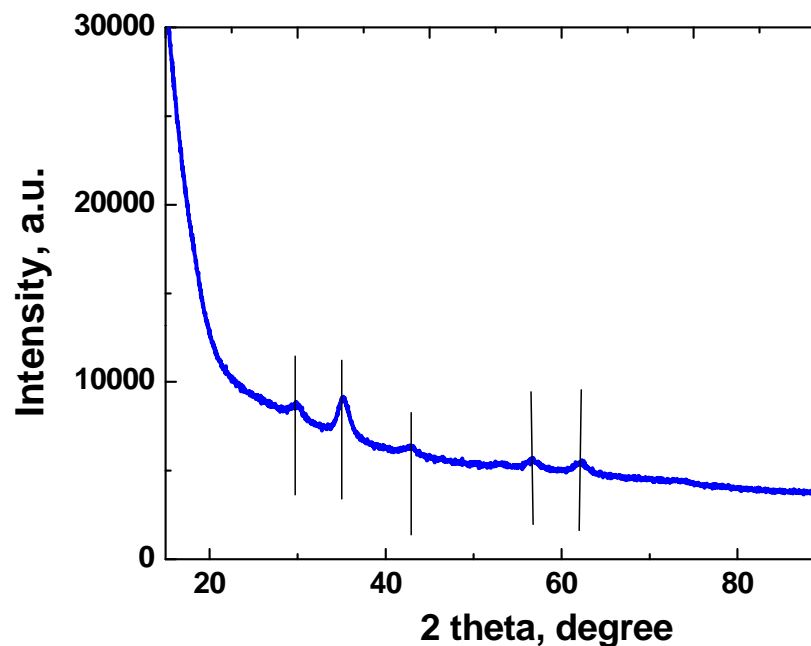
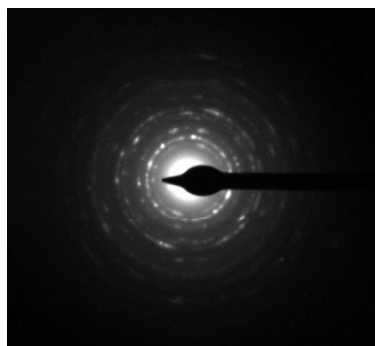
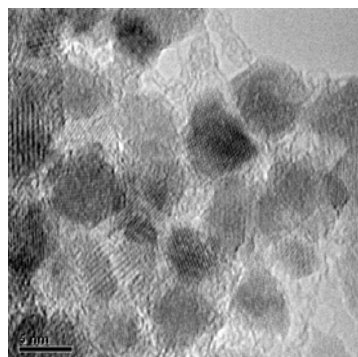
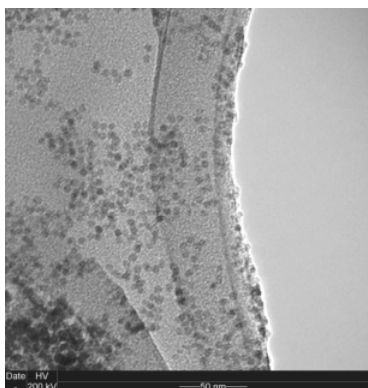
Sun S., Zeng, H., Robinson, D. B., Raoux, S., Rice, P. M., Wang, S. X., Li, G. *J. Am. Chem. Soc.* 2004, 126, 273-279.

# Magnetic Nanoparticle Structure

## WAXS, HR-TEM

Crystalline structure –  $\text{Fe}_2\text{MnO}_4$

Average diameter:  $6.11 \pm 0.69$  nm



	WAXS diffraction Peaks						
	1	2	3	4	5	6	7
d	2.96	2.54	2.11	1.72	1.62	1.49	1.27
$\text{Fe}_2\text{MnO}_4$	2.97	2.54	2.10	1.72	1.62	1.49	1.27
hkl	220	311	400	422	511	440	622

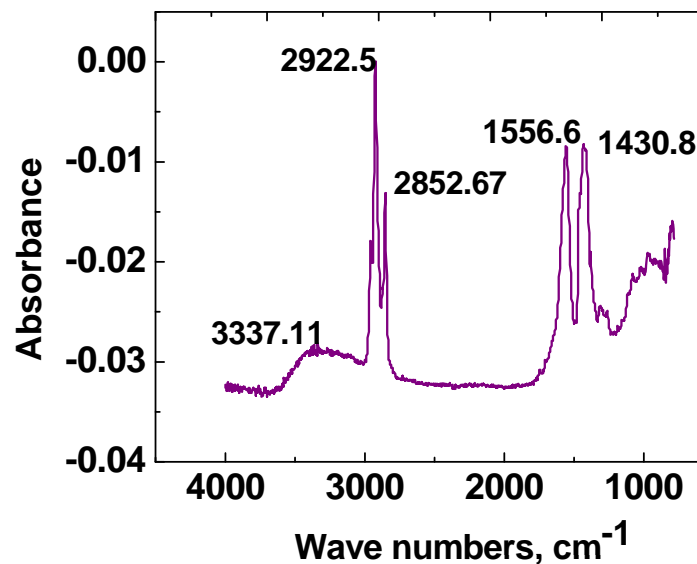
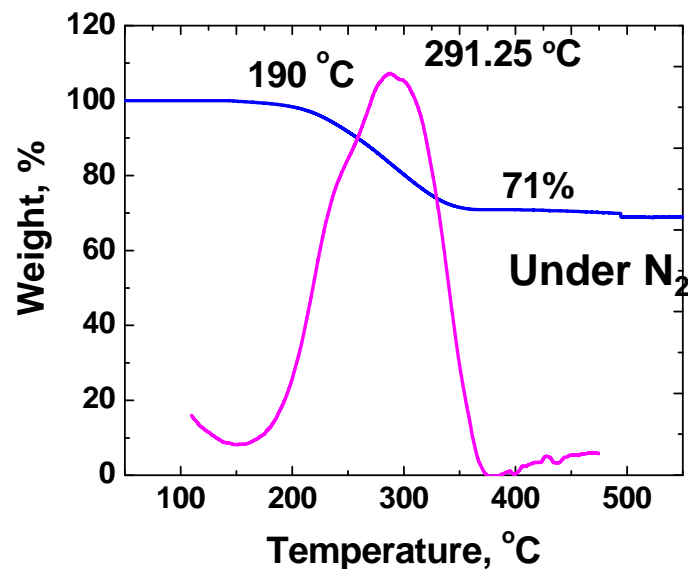
# Surface Characteristics of Iron Manganese Oxide Nanoparticles

## Presence of aliphatic hydrocarbon surface modifier:

TGA : ~ 29% organic surface modifier

IR :

- Hydroxyl group, -OH (3337.11,  $\text{cm}^{-1}$ )
- Aliphatic hydrocarbon chain, -CH stretch in C-CH<sub>3</sub> and -CH<sub>2</sub> (2922.5 and 2852.67  $\text{cm}^{-1}$ )
- Aliphatic hydrocarbon chain, -CH bending stretches (1430.8 and 1556.6  $\text{cm}^{-1}$ )

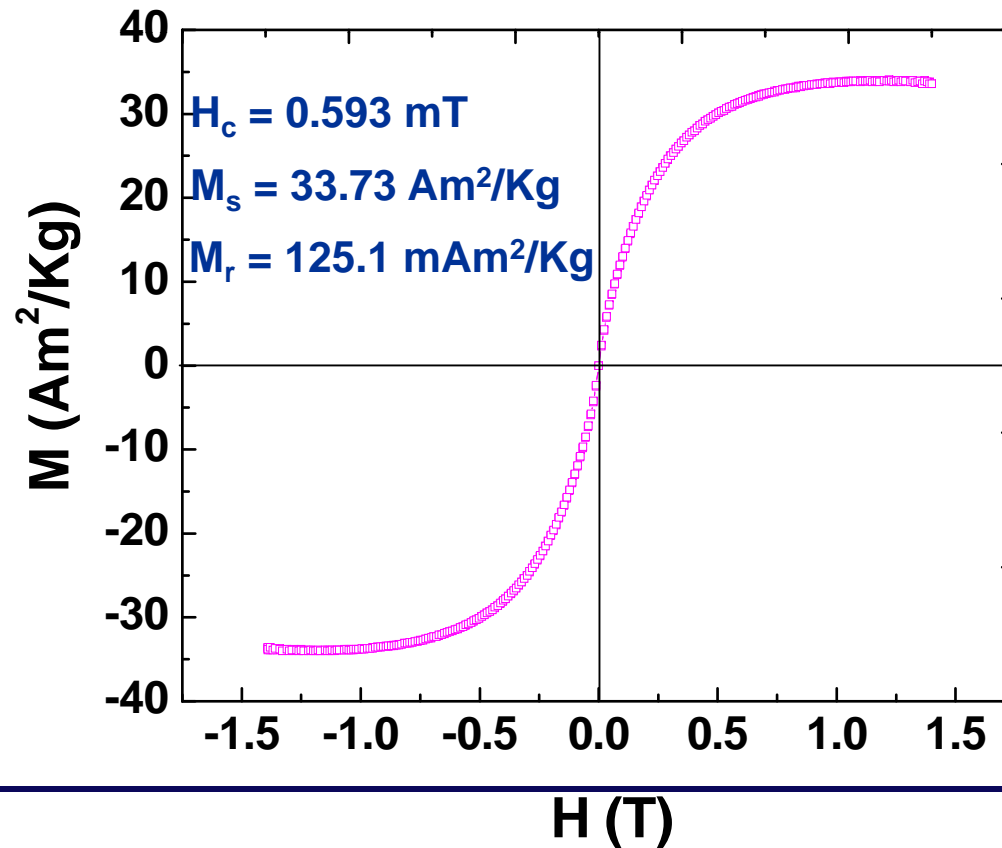


## Super paramagnetic Nanoparticles

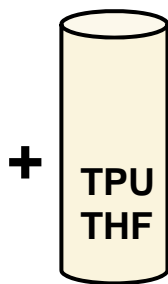
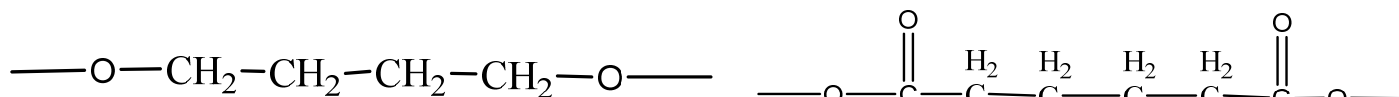
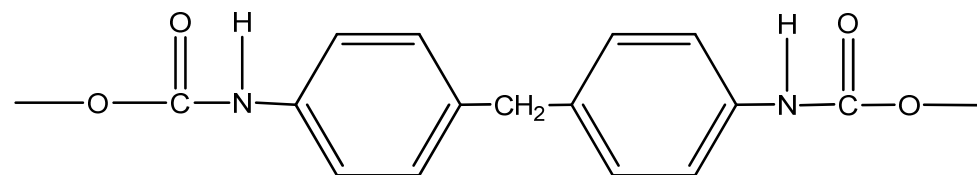
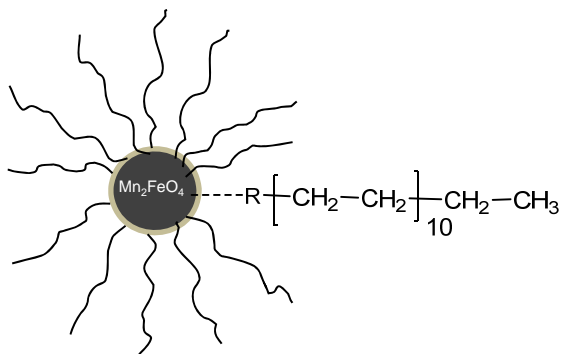
### AC field gradient magnetometer.

The magnetic hysteresis loop was generated by increasing magnetic field up to +1.4T after demagnetization. Then, it was decreased to -1.4T and repeated to generate the curve.

- The saturation magnetization,  $M_s$ , is the magnetic moment of elementary atoms per unit weight where all the dipole are aligned parallel.
- The reverse magnetic field required to reduce the magnetization of materials to zero after a magnetic field is applied called coercivity.



# TPU/Magnetic Nanoparticle Nanocomposites



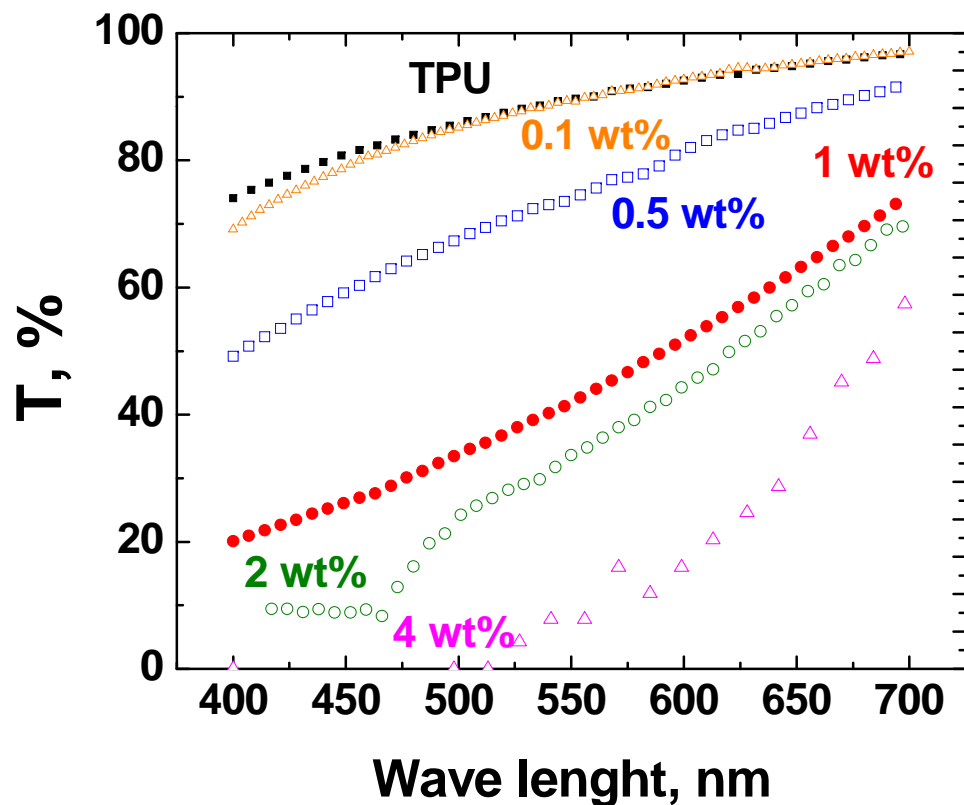
→  
Mild bath sonication



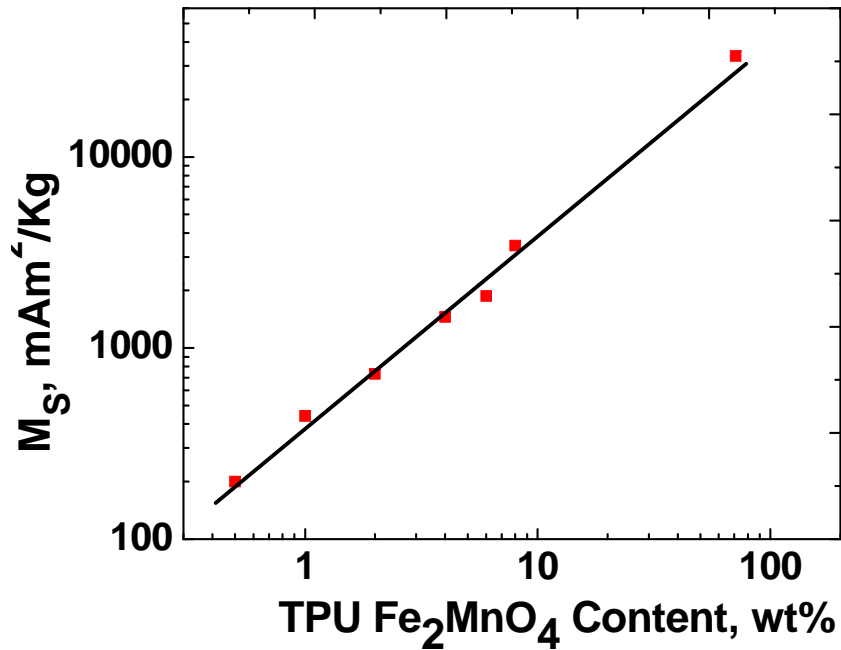
Uniform dispersion of MNP in THF

# Transparency UV-Vis Spectroscopy

$\text{Fe}_2\text{MnO}_4$ /TPU nanocomposite films were transparent < 1wt% and semi-transparent up to 2 wt%.



# Magnetization of Nanocomposites



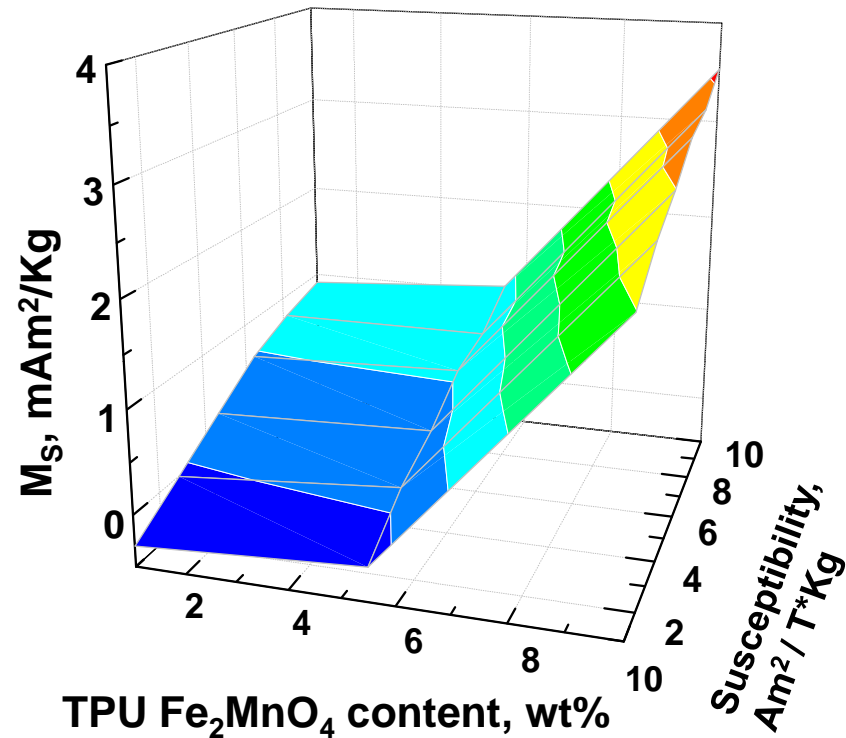
$$M_s = A W^B$$

$$A = 380.19 \pm 0.033,$$

$$B = 10.47 \pm 0.038 \quad (R^2 = 0.99)$$

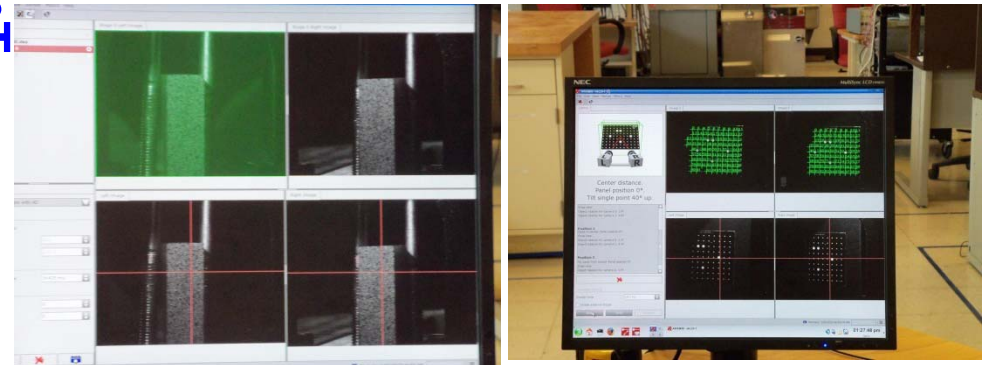
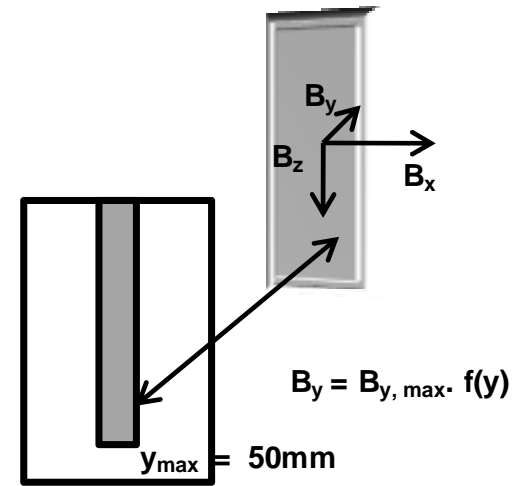
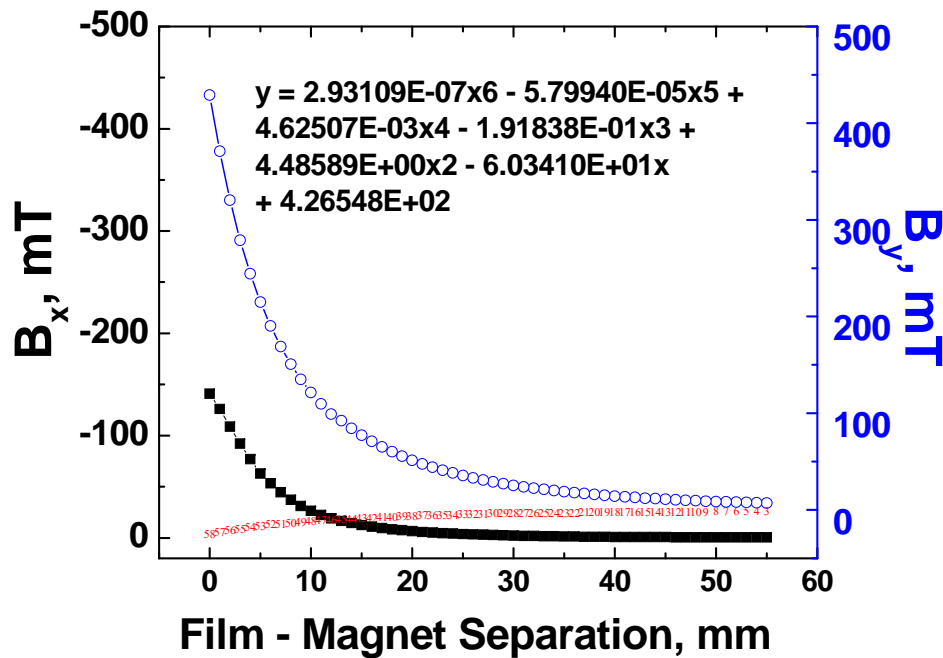
If normalized w/r to weight of nanoparticles:

$$H_c = 0.8 \pm 0.1 \text{ mT}, \quad M_s = 0.04 \pm 0.01 \text{ mAm}^2/\text{Kg}.$$



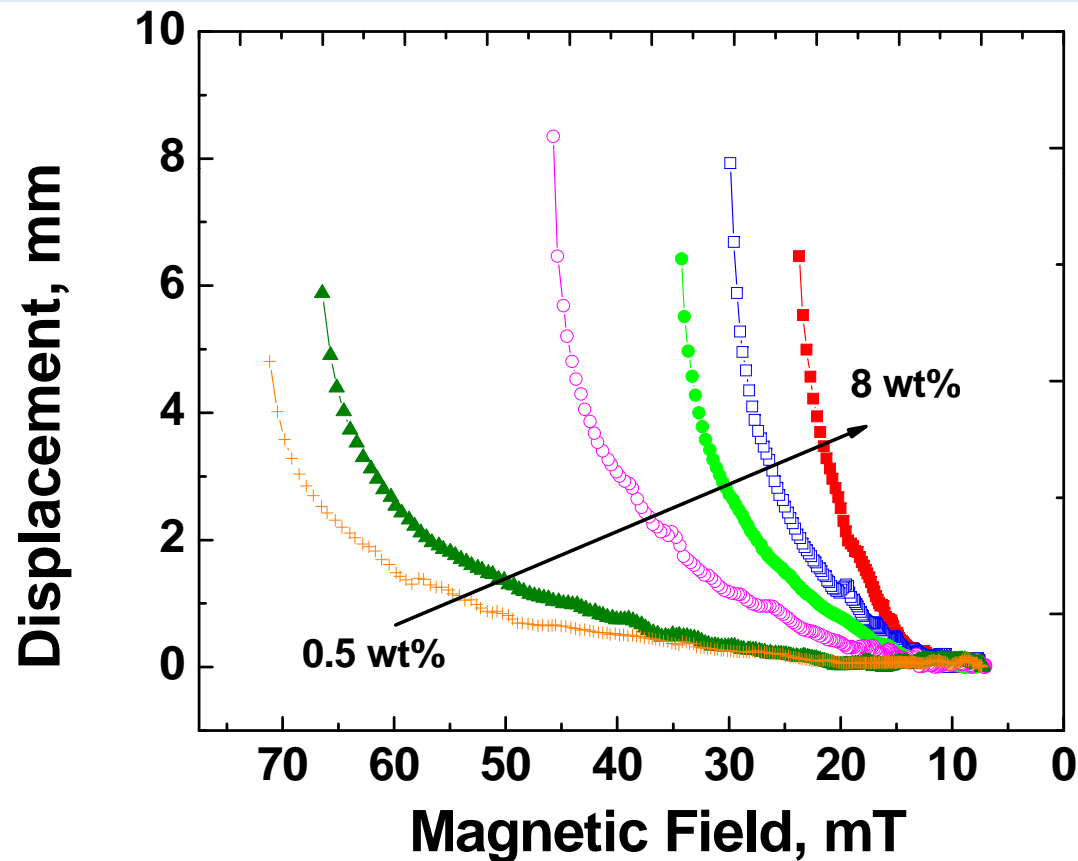
# Magneto-Mechanical Measurements

Actuation measurements were performed using Tytron 250 MTS instrument using MTS Flex Test software and controlled stroke mode at a rate of 1.00 mm/s. Aramis<sup>®</sup> software was used where eight images per stroke were captured. A static magnet with strength of 0.43 T ( $B_y$  ( $z=0$ )) was used.



# Magneto-Mechanical Measurements

Nanocomposites with lower magnetic nanoparticle content exhibited slower deformation rate, meanwhile nanocomposites with high magnetic content ( $> 4\text{wt}\%$ ) showed a faster deformation rate.

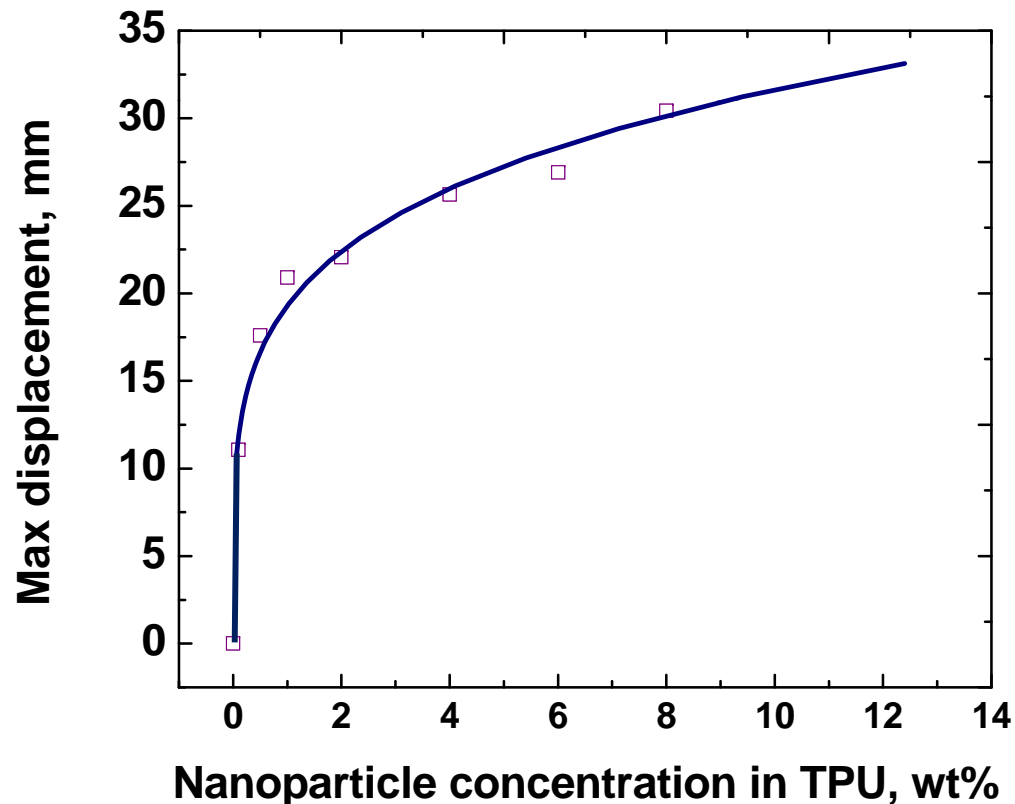


Film displacement as a function of magnetic field strength

# Magneto-Mechanical Measurements

## Maximum Film Displacements

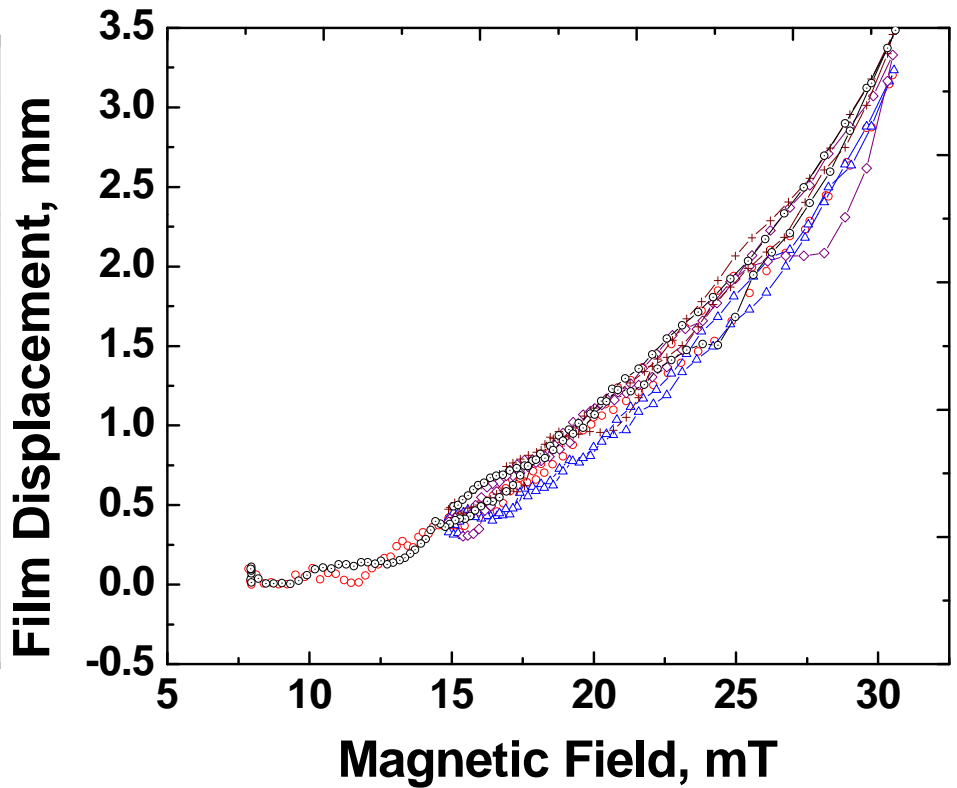
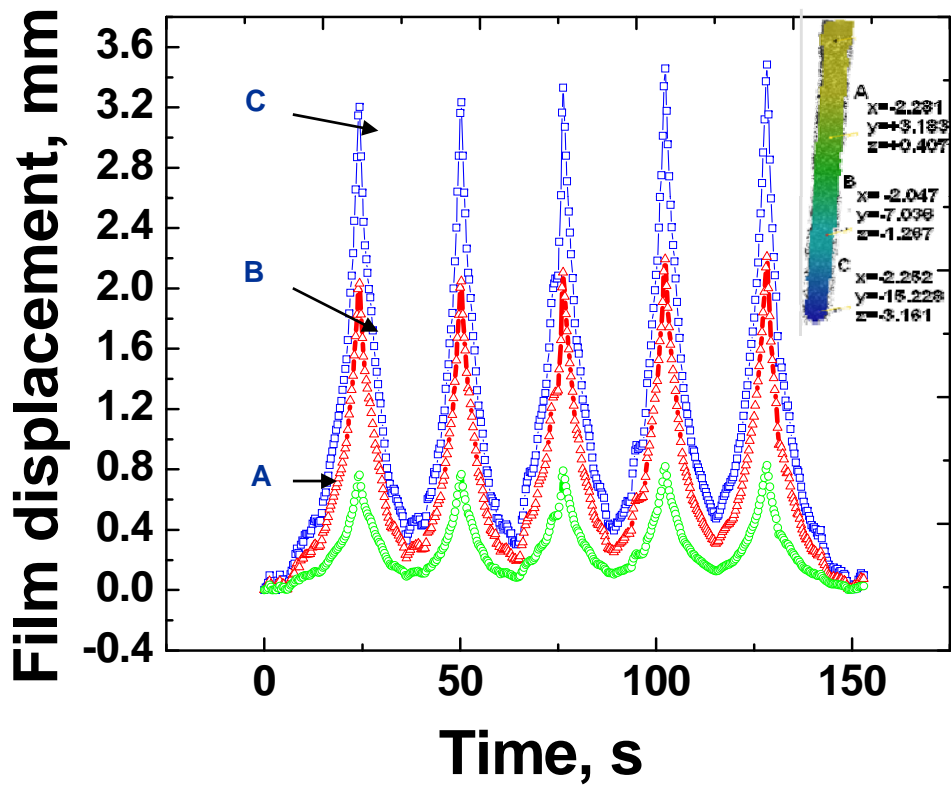
Large deformation  $> 10$  mm was obtained for a nanocomposite containing only 0.1wt% (0.025 vol.%) MNPs. The maximum deformation increased with increasing concentration exponentially.



# Control of Actuation and Repeatability



Highly repeatable with minimal difference in the deformation. The deformation increased from 1<sup>st</sup> cycle to the 5<sup>th</sup> cycle by 8.7%.

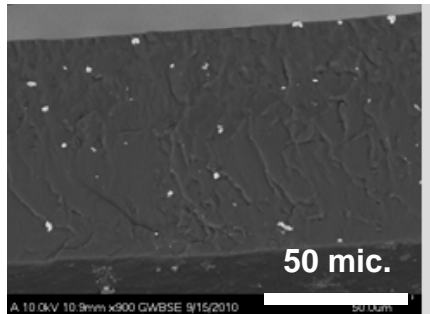


$$7.9529 < B(y) < 15.4619 \text{ (mT)}$$

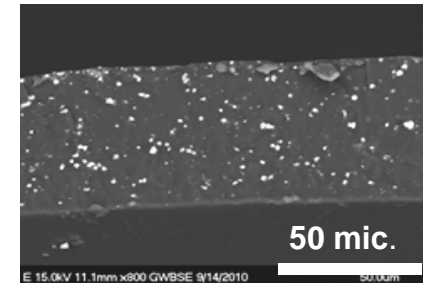
# Morphology SEM / HR-TEM



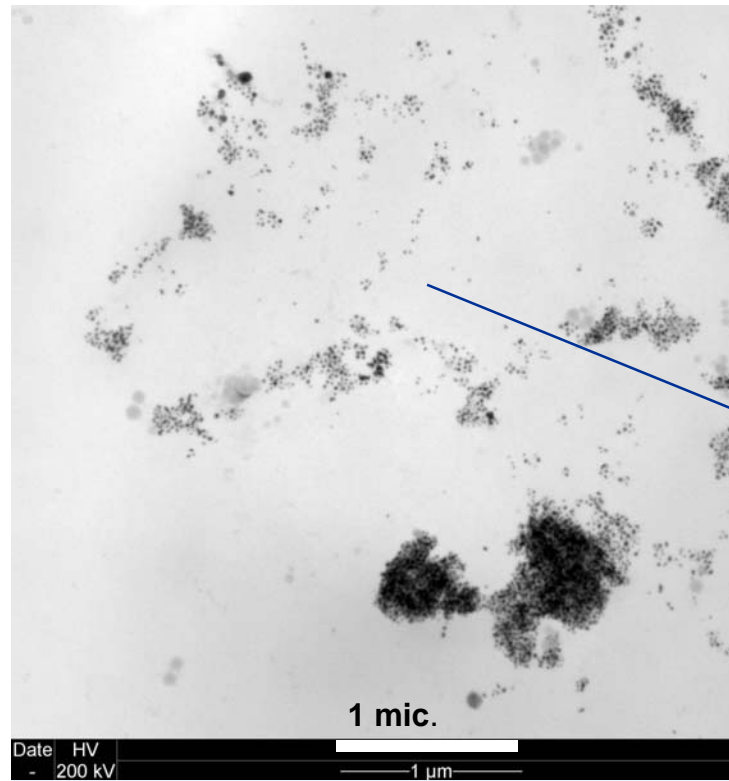
Cryo-fractured surfaces were exposed to oxygen plasma and then bright-field micrographs were collected.



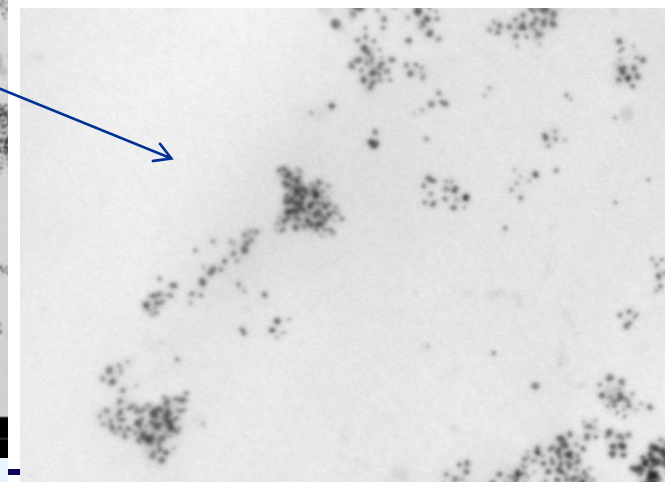
**0.5 wt% MNP/TPU  
nanocomposites**



**6 wt% MNP/TPU  
nanocomposites**



**2 wt% MNP/TPU nanocomposites**

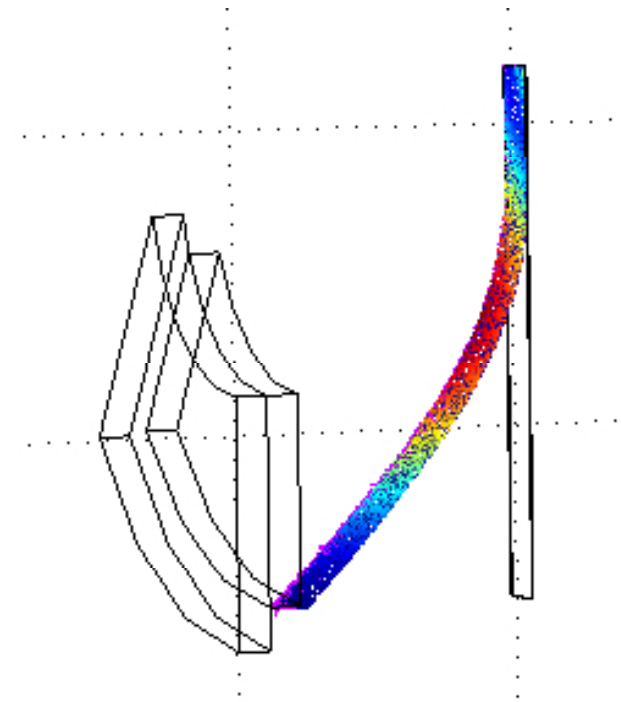
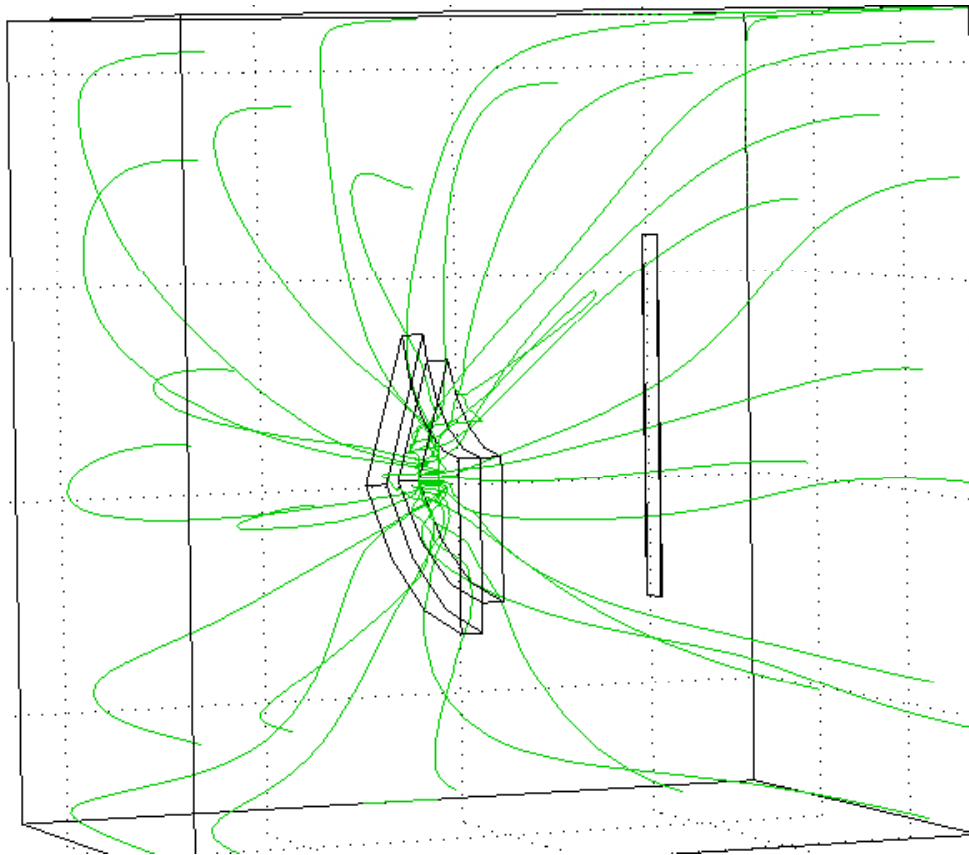




# Magneto-Static Simulations

Simulating the motion of the film upon the application of a magnetic field involves:

- A (linear) stress-strain constitutive model for the composite film
- The magnetostatics equations (including constitutive models for the magnetic behavior of all materials involved in the system, including the surrounding air)
- A deforming mesh for the film, allowing the “domain” to move.





# Magneto-Static Simulations

**Magnetostatics: the magnetic field is steady or quasi-steady (slow changes with respect to time) and there are no electric currents.**

$$\nabla \times \mathbf{H} = 0$$

Magnetic field

$$\mathbf{H} = -\nabla V_m$$

Scalar magnetic potential

$$\mathbf{B} = \mu_0(\mathbf{H} + \mathbf{M})$$

Magnetization

$$\nabla \cdot \mathbf{B} = 0$$

Magnetic flux density

Magnetic permeability of air

$$\mathbf{B} = \mu_0(\mathbf{H} + \mathbf{M})$$

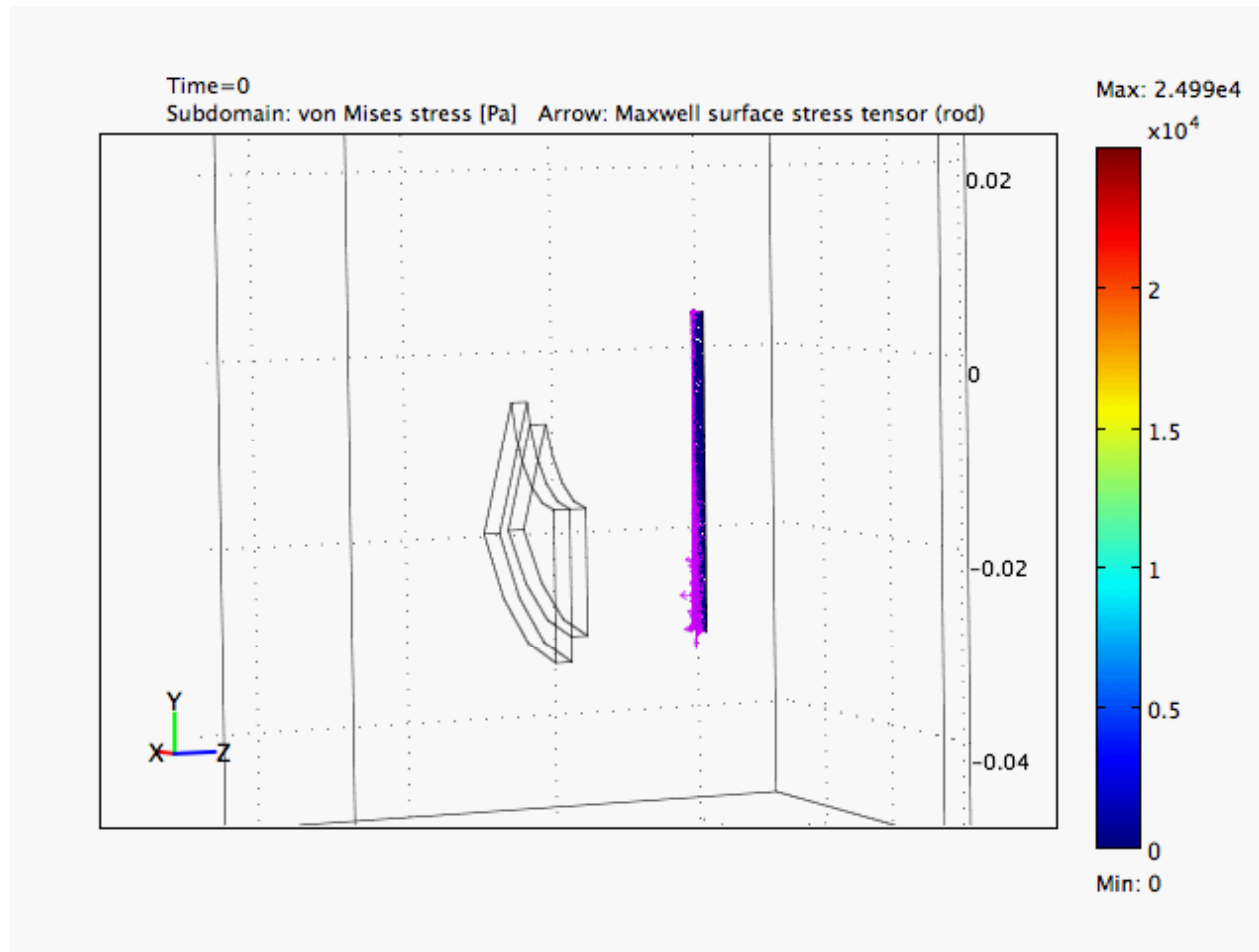
For the permanent magnet:

Everything else (air, backing, film):

$$\mathbf{B} = \mu_0\mu_r\mathbf{H}$$

Relative permeability

# Magneto-Static Simulations



# Conclusions

- **Super paramagnetic TPU films were prepared by addition of super-paramagnetic  $\text{Fe}_2\text{MnO}_4$  spherical nanoparticles to TPU (0.1- 8 wt%).**
- **All nanocomposite films exhibited large deformation  $> 10\text{mm}$  in the magnetic field corresponding to the onset of saturation magnetization.**
- **The actuations were demonstrated to be repeatable and controllable in the magnetic field with minimal (8.7%) loss in the deformation and hysteresis.**
- **A mixed dispersion of nano-sized range particles and micron-sized aggregates were observed.**
- **Magneto-static simulations resulted in large deformations which was in agreement with the experimentally observed results.**



# Acknowledgements

- **The NASA Aeronautics-Subsonic Fixed Wing Program is thanked for the funding (contract NNC07BA13B)**
- **Dr. JoAn Hudson, Advanced Materials Research Laboratories (AMRL), Clemson University, SC**
- **Dr. Richard Rogers, GRC**
- **Terry McCue, ASRC, NASA-GRC**
- **Daniel Scheiman, ASRC/NASA-GRC**
- **Matthew Dittler, Stony Brook University, NASA-USRP Intern**